Hecker, Dominik; Wolters, Maik

Working Paper

Nonlinear Estimation of a New Keynesian Model with Endogenous Inflation De-Anchoring

CESifo Working Paper, No. 12280

Provided in Cooperation with:
Ifo Institute – Leibniz Institute for Economic Research at the University of Munich

Suggested Citation: Hecker, Dominik; Wolters, Maik (2025) : Nonlinear Estimation of a New Keynesian Model with Endogenous Inflation De-Anchoring, CESifo Working Paper, No. 12280, Munich Society for the Promotion of Economic Research - CESifo GmbH, Munich

This Version is available at:
https://hdl.handle.net/10419/334636

CES ifo Working Papers

12280
2025

November 2025

Nonlinear Estimation of a New Keynesian Model with Endogenous Inflation De-Anchoring

Dominik Hecker, Maik Wolters

CES ifo

Imprint:

CESifo Working Papers

ISSN 2364-1428 (digital)

Publisher and distributor: Munich Society for the Promotion
of Economic Research - CESifo GmbH

Poschingerstr. 5, 81679 Munich, Germany
Telephone +49 (0)89 2180-2740

Email office@cesifo.de
https://www.cesifo.org

Editor: Clemens Fuest

An electronic version of the paper may be downloaded free of charge
· from the CESifo website: www.ifo.de/en/cesifo/publications/cesifo-working-papers
· from the SSRN website: www.ssrn.com/index.cfm/en/cesifo/
· from the RePEc website: https://ideas.repec.org/s/ces/ceswps.html

Nonlinear Estimation of a New Keynesian Model with Endogenous Inflation De-Anchoring*

Dominik Hecker† and Maik H. Wolters‡

November 20, 2025

Abstract

We estimate a New Keynesian model that allows endogenous transitions between a *target equilibrium*, with inflation fluctuating around the central bank's target and interest rates typically positive, and a *low-inflation equilibrium*, where the effective lower bound binds and de-anchored expectations keep inflation persistently below target. The model is estimated using Bayesian methods, employing an ensemble MCMC sampler with a particle filter to handle nonlinearities. We find that the United States remained in the target equilibrium after the global financial crisis, the euro area transitioned to the low-inflation equilibrium in 2015, with the subsequent inflation surge initiating a return to the target equilibrium in 2021, and Japan entered the low-inflation equilibrium in the early 2000s. Bayes factors strongly favor the equilibrium-transition model over an alternative specification in which the lower bound binds only occasionally and expectations remain anchored.

Keywords: Multiple Equilibria, Nonlinear Estimation, Particle Filter, Deflation, Zero Lower Bound, Natural Interest Rate, Inflation Expectations

JEL-Codes: C51, E31, E43, E52

*We would like to thank Klaus Adam, Gregor Boehl, Benjamin Born, Pablo Cuba-Borda, Laura Gáti, Kevin Lansing, Sebastian Schmidt, Frank Schorfheide, Christian Schröder, and Cajo Ter Braak as well as participants of various conferences and seminars for helpful comments on this paper. We gratefully acknowledge financial support by the Deutsche Forschungsgemeinschaft (DFG) under project number 508470100.

†Kiel University, E-mail: hecker@economics.uni-kiel.de.

‡Kiel University, Kiel Institute, ifo Institute, Institute for Monetary and Financial Stability at Goethe University Frankfurt. E-mail: wolters@economics.uni-kiel.de.

1 Introduction

The global financial crisis of 2008–2009 prompted central banks to lower policy rates to the effective lower bound (ELB). Despite the use of unconventional monetary policy measures, inflation in economies such as the United States and the euro area remained persistently below target. Declining estimates of the natural rate of interest (see, e.g., Holston et al., 2017) heightened concerns that the ELB would bind more frequently, complicating the stabilization of inflation and inflation expectations (see the strategy reviews of the Federal Reserve and the ECB concluded in 2020 and 2021, respectively). In the euro area, de-anchoring of inflation expectations began after the ELB became binding (see, e.g., Nautz et al., 2017; Natoli and Sigalotti, 2018; Corsello et al., 2021; Christoffel and Farkas, 2025), whereas evidence for the United States is less clear (see, e.g., Strohsal et al., 2016; Grishchenko et al., 2019; Fischer, 2023). Japan's experience shows that low interest rates and low inflation can persist for decades.

While global inflation has risen since 2021 the prospect of renewed low-inflation, low-interest-rate episodes remains salient. The increase in natural interest rates observed during the inflation surge appears to have been temporary, and estimates of r^* have largely reverted to the record lows of the previous decade.[1] Using interest-rate derivatives, Cho et al. (2025) estimate that the probability of the U.S. economy returning to the ELB is 9% at medium- to long-horizon. In Switzerland, inflation and the policy rate have already returned to near-zero levels after a mild increase in inflation between 2021 and 2023.

Existing solution algorithms for macroeconomic models with an ELB typically assume an occasionally binding constraint and that long-run inflation expectations remain anchored at the target (e.g., Guerrieri and Iacoviello, 2015; Holden, 2016; Boehl, 2022). Once shocks fade, these models return to the standard steady state, implying that recurrent adverse shocks or highly persistent shock effects are required to generate long spells of low interest rates and low inflation. The same applies to studies that incorporate an occasionally binding ELB in model estimation (e.g., Richter and Throckmorton, 2016; Gust et al., 2017; Kulish et al., 2017; Aruoba et al., 2021; Boehl and Strobel, 2024).

To address these limitations, we estimate a New Keynesian model in which inflation expectations

[1] U.S. estimates based on Laubach and Williams (2003) have declined but remain somewhat above their post-GFC levels, whereas the estimates of Holston et al. (2017) for the United States and the euro area have returned to levels close to the record lows of the previous decade (see `https://www.newyorkfed.org/research/policy/rstar`).

can de-anchor, allowing the economy to transition from a *target equilibrium*, where inflation fluctuates around the target and the policy rate is mostly above the ELB, to a *low-inflation equilibrium*, where inflation remains persistently below target and the ELB binds most of the time. These two equilibria correspond to fluctuations around the two steady states of New Keynesian models with an ELB (e.g., Benhabib et al., 2001a). Crucially, the economy can remain in the low-inflation equilibrium even after shocks have dissipated, provided long-run inflation expectations have fallen below the target.

The model and expectation-formation framework build on Lansing (2021). Agents form expectations as a weighted average of rational-expectations forecasts for the target and low-inflation equilibria, with the weights evolving according to past forecast performance in the sense of Hommes and Brock (1997). The weights can be interpreted as the perceived probabilities that the economy is in each equilibrium. Persistently low inflation raises the weight on the low-inflation equilibrium, potentially de-anchoring expectations from the target and triggering a transition toward the low-inflation equilibrium. Empirical evidence in Carvalho et al. (2023) shows that imperfect information and past forecast errors are central to the formation of long-term inflation expectations. The model also incorporates permanent shifts in the natural rate of interest, which change the frequency and duration of ELB episodes and thereby affect the central bank's ability to stabilize inflation, the likelihood of de-anchoring, and the probability of a transition to the low-inflation equilibrium. This framework is well suited to environments in which the data reflect a mixture of equilibria—as in an incomplete transition to the low-inflation equilibrium—or to episodes in which a prolonged period of low inflation and low interest rates is followed by an inflation surge that lifts inflation expectations, as observed since mid-2021.

We estimate the model for the United States, the euro area, and Japan using Bayesian methods. Given the model's nonlinear structure, the likelihood function is evaluated with the bootstrap particle filter (Herbst and Schorfheide, 2016). This approach is computationally demanding, and the commonly used Random-Walk Metropolis–Hastings algorithm offers limited scope for parallelization. To address this, we implement the Differential-Independence Mixture Ensemble (DIME) sampler developed by Boehl (2024), which builds on the Differential Evolution Markov Chain algorithm of ter Braak and Vrugt (2008), allows for efficient parallel computation and reduces the risk of getting stuck in a local maxima.

Our contribution to the literature is threefold. First, to our knowledge, no previous study has estimated a nonlinear model that allows for endogenous transitions to a low-interest rate and low-inflation equilibrium. Prior work either employs a calibrated equilibrium-transition model (Lansing, 2021), estimates a linear version on a sample excluding the ELB and uses those estimates to parameterize a two-equilibria model (Aruoba et al., 2018), or assumes the economy is permanently in the low-inflation equilibrium so that linear estimation suffices (Cuba-Borda and Singh, 2024). Second, we provide the first application of such a model to the euro area. Earlier studies have focused on the United States (Lansing, 2021), Japan (Cuba-Borda and Singh, 2024), or both (Aruoba et al., 2018). We view the euro area as particularly informative: between 2010 and 2020, the risk of transitioning to the low-inflation equilibrium was arguably greater than in the United States, given the larger decline in inflation and lower long-term inflation expectations. For Japan, by contrast, it is widely acknowledged that the economy has been in the low-inflation equilibrium for many years. Third, we systematically assess the empirical relevance of the equilibrium-transition model by comparing its fit and parameter estimates with those of two single-equilibrium specifications. While both alternatives are considered for all three economies, for the United States and the euro area the target-equilibrium model with anchored long-run inflation expectations and an occasionally binding ELB—that is, a standard New Keynesian model with an ELB—is of primary interest. For Japan, the low-inflation equilibrium, in which expectations are anchored at minus the natural rate and interest rates deviate only temporarily from the ELB, is of primary interest.

We find that the United States remained in the target equilibrium during the post–global financial crisis period of low inflation and interest rates. The euro area transitioned to the low-inflation regime in 2015. As inflation temporarily rose toward target around 2018, the euro area economy was best characterized as a mixture of the target and low-inflation equilibria. Following the inflation surge beginning in 2021, the euro area returned to the target equilibrium. Japan appears to have entered the low-inflation equilibrium in the early 2000s, although estimates are volatile. Until 2013, Japan's inflation target was only 1%, implying a narrow gap between the target and the average inflation rate in the low-inflation equilibrium—estimated as the negative of the natural rate, which was close to zero at the time—making it difficult to distinguish the two equilibria precisely.

Bayes factor and the Kass–Raftery statistic provide strong evidence in favor of the transition-equilibrium specification relative to single-equilibrium specifications across all three economies.

Posterior parameter estimates differ markedly across models, indicating that specifications without equilibrium transitions may yield unreliable estimates when the sample includes extended periods of low inflation and interest rates—even if inflation subsequently returns to target. This point is especially important given that Aruoba et al. (2018) show that dynamics differ substantially between the target and low-inflation equilibria, while Lansing (2021) shows that transitions across equilibria generate dynamics distinct from those in the target equilibrium. Accordingly, policy analyses based on models with anchored expectations and only an occasionally binding ELB may be misleading.

Several papers are closely related to ours. Benhabib et al. (2001a) show that the ELB constraint generates, alongside the standard target steady state, a second steady state in which the ELB binds and inflation equals the negative of the steady-state real interest rate, with an infinite number of equilibrium paths connecting the two. In subsequent work, they demonstrate that a standard Taylor rule cannot rule out convergence to the low-inflation steady state (Benhabib et al., 2001b). We focus on two local equilibria relevant at low interest rates: fluctuations around the target steady state and fluctuations around the low-inflation steady state. In light of the secular decline in the natural rate of interest, the latter is relevant not only for persistent deflation but also for episodes of persistently low but positive inflation.

Theoretical papers study New Keynesian models with target and low-inflation equilibria. For example, Armenter (2018) shows that inflation, price-level, or nominal GDP targeting may not be sufficient to prevent convergence to a low-inflation equilibrium. Mertens and Ravn (2014), Nakata and Schmidt (2022), and Bilbiie (2022) show that policy effects at the ELB depend on whether the liquidity trap is driven by fundamental or non-fundamental shocks. Schmitt-Grohé and Uribe (2017) add downward nominal wage rigidity to a model with non-fundamental traps to explain why ELB recessions often yield jobless recoveries. Christoffel and Farkas (2025) develop a model in which inflation expectations may de-anchor and agents update a time-varying perceived inflation target from past inflation outcomes, though they do not consider the low-inflation equilibrium that is the focus of this paper.

Empirical work on two-equilibria models is more limited. Aruoba et al. (2018) examine whether the liquidity traps in the United States and Japan are driven by non-fundamental shocks that induce switches to a low-inflation equilibrium, or by adverse fundamental shocks generating temporary

ELB episodes with expectations anchored at the target. They solve a nonlinear model with global methods and use a particle filter to recover the sequence of shocks consistent with the data, estimating the probability of being in each equilibrium. Consistent with our results, they find that the United States likely remained in the target equilibrium, while Japan switched to the low-inflation equilibrium. In their framework, transitions occur exogenously via sunspot shocks. Lansing (2021) instead allows for endogenous equilibrium switching. He finds that the probability of the target equilibrium declines for the U.S. economy after the global financial crisis but remains above 50 percent by the end of the sample in 2018, and in one specification stays near one—again in line with our findings. Cuba-Borda and Singh (2024) distinguish between non-fundamental expectations-driven and secular stagnation liquidity traps for Japan, where the latter involves a permanent decline of the natural rate below zero, and find stronger support for the expectations-driven case. Fischer (2023) estimates a model in which agents switch endogenously between constant-gain learning and random-walk forecasts. He finds that de-anchoring can generate deflationary spirals when the ELB binds and evaluates policy measures to prevent such outcomes.

The remainder of the paper proceeds as follows. Section 2 introduces the model with two equilibria and describes the transition mechanism. Section 3 describes the estimation methodology. In Section 4 the estimation results and equilibrium probabilities are discussed. Section 5 compares the transition model to single-equilibrium models. Section 6 shows robustness checks. Finally, Section 7 concludes.

2 Model Environment

We employ a small-scale New Keynesian model with an ELB constraint. This choice offers three advantages over larger-scale models. First, the framework is well established in the literature, which facilitates a clear analysis of how allowing for equilibrium transitions alters the model's dynamics. Second, the small number of state variables substantially reduces the computational burden associated with solving and estimating the model. Third, endogenous transitions between target and low-inflation equilibria can generate richer dynamics, in which case the additional frictions embedded in larger models may be unnecessary for matching the data.

2.1 Core Model Equations

The IS curve in equation (1) can be derived from the consumption Euler equation, while the Phillips curve in equation (2) follows from the profit-maximization problem of firms operating under monopolistic competition and subject to price-setting frictions:

$$y_t = \hat{E}_t y_{t+1} - \alpha(i_t - \hat{E}_t \pi_{t+1} - r_t) + v_t, \tag{1}$$

$$\pi_t = \beta \hat{E}_t \pi_{t+1} + \kappa y_t + u_t. \tag{2}$$

Here, y_t denotes the output gap, π_t the quarterly inflation rate, i_t the nominal interest rate, and r_t the short-run natural interest rate. The operator $\hat{E}_t$ represents expectations formed by agents who account for the possibility that the economy may transition between the target and low-inflation equilibria. The specific expectation-formation mechanism is described below.

The supply shock u_t and demand shock v_t are modeled as first-order autoregressive processes, with persistence parameters ρ_u and ρ_v, respectively. The innovations, $\epsilon_{u,t}$ and $\epsilon_{v,t}$, are assumed to be mean-zero and normally distributed with variances $\sigma^2_{\epsilon_u}$ and $\sigma^2_{\epsilon_v}$:

$$u_t = \rho_u u_{t-1} + \epsilon_{u,t}, \tag{3}$$

$$v_t = \rho_v v_{t-1} + \epsilon_{v,t}. \tag{4}$$

Unlike standard frameworks, the natural interest rate is allowed to vary in the long run. The long-run natural rate, r^*_t, follows a random walk, while the short-run natural rate, r_t, is a weighted average of its lagged value and the long-run rate:

$$r^*_t = r^*_{t-1} + \eta_t, \tag{5}$$

$$r_t = \rho_r r_{t-1} + (1 - \rho_r) r^*_t + \epsilon_t. \tag{6}$$

The shocks η_t and ϵ_t are mean-zero and normally distributed with variances σ^2_η and σ^2_ϵ, respectively, generating permanent or temporary fluctuations in the natural interest rate.

The central bank sets the nominal interest rate according to a policy rule subject to the ELB,

which is assumed to be zero:

$$i_t = \max\{0, \rho i_{t-1} + (1-\rho)(r_t + \pi^* + g_\pi(\bar{\pi}_t - \pi^*) + g_y y_t)\}, \tag{7}$$

$$\text{with} \quad \bar{\pi}_t = \omega \pi_t + (1-\omega)\bar{\pi}_{t-1}, \tag{8}$$

where π^* denotes the inflation target, and ω is calibrated so that the exponentially weighted average $\bar{\pi}_t$ of current and past quarterly inflation approximates the four-quarter compound inflation rate. A permanent decline in r_t^* , and consequently in r_t, increases the frequency with which the ELB binds.

2.2 Two Local Equilibria

The long-run Fisher relation is embedded in equation (1), so that if the Taylor principle is satisfied, the model features two long-run endpoints corresponding to the steady states of New Keynesian models with an ELB, as first described by Benhabib et al. (2001a). Because the long-run natural interest rate r_t^* is nonstationary, the model does not admit a true steady state, but only long-run endpoints, in which some variables depend on r_t^*. At the target long-run endpoint, inflation is equal to its target and the nominal interest rate is positive: $\pi_t^T = \pi^*$, $i_t^T = r_t^* + \pi^*$, and $y_t^T = (1-\beta)\pi^*/\kappa$. At the low-inflation endpoint, inflation is below target and the ELB binds: $\pi_t^L = -r_t^*$, $i_t^L = 0$, and $y_t^L = (1-\beta)(-r_t^*)/\kappa$.

We focus on two local rational expectations equilibria corresponding to the long-run endpoints. In the *target equilibrium*, agents' long-run expectations are anchored at the target endpoint. Inflation fluctuates around the inflation target, and the nominal interest rate remains mostly positive. Expectations in this equilibrium are denoted $\hat{E}_t^T$ and are computed under the assumption that the ELB never binds, allowing the use of standard rational expectations solution methods.

In the *low-inflation equilibrium* equilibrium, agents' long-run expectations are anchored at the low-inflation endpoint. Expectations in this equilibrium are denoted $\hat{E}_t^L$ and are computed under the assumption that the ELB is permanently binding.[2] The Blanchard-Kahn conditions do not hold. However, by redefining the inflation expectational error as an additional fundamental variable,

[2]See Lansing (2021) for a discussion showing that computing expectations under the assumption that the ELB never binds in the target equilibrium and always binds in the low-inflation equilibrium is unproblematic, as simulations indicate these assumptions are only rarely and briefly violated.

following Farmer et al. (2015), the solution becomes non-explosive, and standard solution methods can be applied. In this equilibrium, inflation fluctuates around minus the long-run natural interest rate, and in simulations the ELB binds for most periods.

2.3 Expectation formation and equilibrium transitions

In the full model, the data are generated by a time-varying mixture of the two local equilibria. Let $x_t \equiv [y_t, \pi_t]$ denote the vector of variables for which expectations must be formed, and let $\hat{E}_t^T x_{t+1}$ and $\hat{E}_t^L x_{t+1}$ denote expectations under the target and low-inflation equilibria, respectively. The expectations $\hat{E}_t$ entering the IS curve (1) and the Phillips curve (2) are then a weighted average of the two equilibria, with the weight on the target equilibrium denoted $\mu_t \in [0, 1]$:

$$\hat{E}_t x_{t+1} = \mu_t \hat{E}_t^T x_{t+1}^T + (1 - \mu_t)\hat{E}_t^L x_{t+1}^L. \tag{9}$$

Following Lansing (2021), we assume that agents update the weight μ_t each period based on the past forecasting performance of the target and low-inflation expectations. Specifically, they choose μ_t to minimize the root mean squared forecasting error of inflation and output gap expectations over the previous T_w quarters:

$$\mu_t = \arg\min_{\mu_t} \sum_{k=1}^{T_w} \left\{ T_w^{-1} \sum_{x \in \{y,\pi\}} \left[x_{t-k} - \left(\mu_t \hat{E}_{t-k-1}^T x_{t-k} + (1 - \mu_t)\hat{E}_{t-k-1}^L x_{t-k} \right) \right]^2 \right\}^{0.5}, \tag{10}$$

If agents observe that their past forecasts perform relatively poorly compared with the ex-post realizations of x_t, they assign more weight to the other equilibrium. In this sense, μ_t can be interpreted as the subjective probability that agents assign to the target equilibrium, with $1 - \mu_t$ representing the probability assigned to the low-inflation equilibrium.

3 Estimation Setup

We estimate the equilibrium transition model using Bayesian methods for the United States, the euro area, and Japan, and we also estimate single-equilibrium models separately for comparison.

3.1 Data and Calibration

We use quarterly data on inflation, the output gap, the policy rate, and the long-run natural real rate of interest, so that π_t, y_t, i_t, and r_t^* are the observables. Sample periods differ across the United States, the euro area, and Japan due to data availability.

For the United States, we use PCE inflation, the output gap based on the Congressional Budget Office's potential output estimates, the effective federal funds rate, and the natural interest rate estimates of Laubach and Williams (2003). The sample runs from 1988Q1 to 2023Q4, the last date for which natural rate estimates are available.

For the euro area, we use inflation based on the Harmonized Index of Consumer Prices, the output gap based on the European Commission's potential output estimates, the ECB's main refinancing operations rate, and the natural interest rate estimates of Holston et al. (2017). The sample runs from 1999Q1 to 2023Q3.

For Japan, we use CPI inflation, the Bank of Japan's output gap estimates, the Bank of Japan's basic discount rate, and the natural interest rate estimates of Nakano et al. (2024), who apply the methodology of Laubach and Williams (2003). The availability of the natural rate series restricts the sample to 1985Q1–2023Q1.

We calibrate some parameters prior to estimation. The discount factor β is set to 0.99 for all three economies. The weighting parameter ω is chosen to minimize the squared distance between the exponentially weighted moving average of quarterly inflation, $\bar{\pi}_t$, and the comparable four-quarter inflation series for each country, as in Lansing (2021). The values of ω are 0.42 for the United States, 0.48 for the euro area, and 0.37 for Japan. For the United States and the euro area, the inflation target is $\pi^* = 2\%$. The Bank of Japan increased its inflation target in January 2013 from 1% to 2%. Implementing a time-varying inflation target would complicate the solution, so we use an average target of 1.26% for the whole sample. We view this approach as reasonable because, until the recent inflation surge, inflation remained not only below the new target level but also below the old one.

3.2 Priors

We establish prior distributions for the parameters to be estimated—α, κ, ρ, g_π, g_y, ρ_u, ρ_v, σ_u, σ_v, ρ_r, σ_ϵ, and σ_η—drawing on those used in the influential study by An and Schorfheide (2007), which employs a model similar to the target equilibrium version of the model used here. The priors are reported in Table 1.

The prior for α, the intertemporal elasticity of substitution, is centered at 0.5 a standard value in the literature. The prior for the Phillips curve slope, κ, is set at 0.2, reflecting micro-level evidence on the frequency of price adjustments. Priors for the policy rule coefficients are loosely centered on the parameters of a Taylor rule with moderate interest rate smoothing. All priors are intentionally broad, allowing the same set to be applied across all three economies.

Table 1: Prior Distributions

Parameter	Domain	Distribution	Para (1)	Para (2)
α	[0, 2.5)	$\mathcal{G}$	0.50	0.50
κ	[0, 2.5)	$\mathcal{G}$	0.20	0.10
g_π	[1, 2.5)	$\mathcal{G}$	1.50	0.25
g_y	[0, 2.5)	$\mathcal{G}$	0.50	0.25
ρ	[0, 1.0)	$\mathcal{B}$	0.50	0.20
ρ_u	[0, 1.0)	$\mathcal{B}$	0.50	0.20
ρ_v	[0, 1.0)	$\mathcal{B}$	0.50	0.20
σ_u	[0, 0.1)	$\mathcal{IG}$	0.10	2.00
σ_v	[0, 0.1)	$\mathcal{IG}$	0.10	2.00
ρ_r	[0, 1.0)	$\mathcal{B}$	0.50	0.20
σ_ϵ	[0, 0.1)	$\mathcal{IG}$	0.10	2.00
σ_η	[0, 0.1)	$\mathcal{IG}$	0.10	2.00

Notes: The prior distribution types are abbreviated as Gamma ($\mathcal{G}$), Beta ($\mathcal{B}$), and Inverse Gamma ($\mathcal{IG}$). Para (1) and Para (2) list the mean and standard deviation for the Gamma and Beta distributions, respectively. For the Inverse Gamma distribution, Para (1) denotes the shape parameter and Para (2) the scale parameter.

We impose an upper bound of 2.5 on the parameters α, κ, g_π, and g_y, as values above this threshold are uncommon in similar estimation studies. For the interest rate smoothing coefficient, ρ, the upper bound is set to 1.0. These constraints are intended to guide the sampler toward regions of the parameter space with higher posterior likelihood and to avoid exploration of areas considered a priori implausible.

We constrain the autoregressive coefficients of the shock processes to lie between 0 and 1 to ensure model stability. To reflect this constraint, we chose a beta distribution that assigns positive weight only within this interval. We use a prior mean of 0.5 and a prior standard deviation of 0.2.

For the standard deviations of the shocks, we use inverse gamma distributions, as they assign positive probability only to positive values. We set the prior shape parameter to 0.1 and the scale parameter to 2.0. These priors for the autoregressive processes and shock variances are standard in the literature (e.g., Smets and Wouters, 2007).

3.3 Particle Filter

To estimate the model, we write it in state-space form. The measurement equation (11) relates the observed time series, Y_t, to the states, X_t, where the measurement function H depends on the parameter vector θ. The transition equation (12) describes the evolution of the states over time, depending on the transition function F, the parameter vector θ, the previous state X_{t-1}, and the structural shocks W_t:

$$Y_t = H(X_t; \theta), \tag{11}$$

$$X_t = F(X_{t-1}, W_t; \theta). \tag{12}$$

Note that, unlike the standard approach, variables are not measured as deviations from a steady state, since the model has no single steady state but two long-run endpoints. Consequently, the model variables are defined directly in levels, as in the data. The measurement equations therefore do not include any steady-state values. They link the model variables directly to the data without transformation, and we also refrain from modeling measurement errors:

$$\pi_t^{data} = \pi_t, \quad y_t^{data} = y_t, \quad i_t^{data} = i_t, \quad r_t^{*,data} = r_t^*. \tag{13}$$

It is noteworthy that H and F in equations (11) and (12) are not necessarily linear. In our case, the function F captures the relevant nonlinearities and the multiple equilibria.

The likelihood function cannot be evaluated analytically because the model's nonlinearity prevents the use of the Kalman filter. To address this, we approximate the likelihood using a particle filter. The particle filter is a Monte Carlo–based algorithm that estimates the likelihood by simulating a *swarm* of particles, each representing a possible state of the system. By iteratively updating the particle weights, the particle filter provides an efficient approximation of the likelihood, en-

abling estimation of the posterior distribution via Bayes' theorem. The application of particle filters to DSGE models was pioneered by Fernández-Villaverde and Rubio-Ramírez (2007), with a comprehensive overview provided by Herbst and Schorfheide (2016).

The particle filter begins by sampling particles from the prior distribution. At each time step, it propagates these particles forward according to the state transition equation, reweights them based on the likelihood of the observed data, and resamples to avoid weight degeneracy. This procedure produces an evolving empirical approximation to the filtering distribution of the latent state, with high-weight particles contributing more to the approximation. With enough particles, the particle filter provides an accurate approximation to the posterior distribution of the state.

We use in the following the bootstrap particle filter as proposed in Herbst and Schorfheide (2019) with $N = 10,000$ particles.

3.4 Adaptive MCMC Algorithm

The Random Walk Metropolis-Hastings (RWMH) algorithm, commonly used to simulate the posterior distribution in DSGE model estimation, is not feasible here due to its slow convergence. Running multiple chains in parallel is a potential alternative. However, independent chains may converge to the same mode, which need not be the global maximum of the posterior likelihood.

We therefore use the differential-independence mixture ensemble (DIME) sampler developed by Boehl (2024), which overcomes the slow convergence and inefficient parallelization of the RWMH algorithm and avoids getting stuck in local maxima. It achieves this through an ensemble sampler approach, running multiple adaptive chains in parallel that are interdependent. The DIME algorithm combines differential evolution with a mixture model for parameter estimation, resulting in superior performance compared with RWMH, with the differential evolution step further enhancing its efficiency.

The DIME sampler uses an ensemble $\Theta_i = (\theta_i^1, \ldots, \theta_i^{n_c})$ of n_c individual chains θ_i^j. The ensemble is initialized with n_c draws from the prior distribution. In each iteration, the algorithm divides the ensemble into two subensembles, which are updated sequentially, with each conditioned on the current state of the other. This structure allows the chains within each subensemble to be processed in parallel. At each iteration, the algorithm employs a mixture of strategies, assigning each chain

to either a local or a global transition kernel with probabilities ξ and $1 - \xi$, respectively.

When a chain j is assigned to the local kernel, its parameter vector θ_i^j is updated using the Differential Evolution Monte Carlo (DEMC) step originally proposed by ter Braak and Vrugt (2008). The DEMC step generates new candidate vectors by taking differences between existing vectors and adding them to the current position of the chain. Specifically, at each iteration i, the indices of two other chains, k and l ($k \neq l \neq j$), are randomly drawn, and the difference between their parameter vectors is weighted by γ and added to the current vector θ_{i-1}^j, along with a small noise term ϵ_i^j:

$$\theta_i^j = \theta_{i-1}^j + \gamma(\theta_{i-1}^k - \theta_{i-1}^l) + \epsilon_i^j. \tag{14}$$

This produces a new parameter vector that depends on the previous position of chain j and information from the current positions of chains k and l. As the ensemble approaches the posterior distribution, the proposal distribution adapts accordingly and converges, too. The DEMC step has been shown to be effective for sampling from high-dimensional and multimodal distributions.

In the case of the global transition kernel, the new draw for θ_i^j depends not on the current positions of two other chains, but on the history and current positions of the entire ensemble. This ensures that the algorithm does not get stuck in a local maximum, but can explore the sampling space more broadly. The new draw is sampled from a proposal distribution that is independent yet adaptive, adjusting over time to approximate the current estimate of the posterior distribution. Specifically, θ_i^j is drawn from a multivariate t-distribution, which can be parametrized in terms of its mean and covariance when the degrees of freedom ν are larger than two:

$$\theta_i^j \sim t_\nu \left(\mu_i, \Sigma_i\right). \tag{15}$$

The multivariate mean μ_i and covariance matrix Σ_i of the distribution do not depend on a single chain, but on the entire ensemble and are updated according to:

$$\mu_i = \left(\frac{W_{i-1}}{W_i}\right) \mu_{i-1} + \left(\frac{w_i}{W_i}\right) \bar{\mu}_i, \tag{16}$$

$$\Sigma_i = \left(\frac{W_{i-1}}{W_i}\right) \Sigma_{i-1} + \left(\frac{w_i}{W_i}\right) \bar{\Sigma}_i, \tag{17}$$

where $\bar{\mu}_i$ and $\bar{\Sigma}_i$ denote the sample mean and covariance matrix of the current ensemble Θ_i, respectively. Within this updating scheme, W_i evolves as:

$$W_i = \rho W_{i-1} + w_i, \tag{18}$$

where ρ is a decay parameter close to unity to ensure the boundedness of W_i and the weight in iteration i is defined as:

$$w_i = a_i \sum_{j=1}^{nc} \pi(\theta_i^j), \tag{19}$$

with a_i being the average acceptance ratio in i and π representing the likelihood function.

After generating a new parameter vector θ_i^j using either the local or global transition kernel, each chain j undergoes a standard Metropolis step. The algorithm then proceeds by assigning a new local or global kernel. Upon convergence, the joint distribution of all chains, i.e., the entire ensemble, represents the posterior distribution.

Test runs of the DIME algorithm revealed an insufficient parameter space exploration with median posterior estimates often on the prior bounds. These issues relate to the DIME algorithm applying a logistic mapping between the constrained parameter space and the unconstrained proposal space. Particularly when the supported parameter space is narrow, the transformation becomes very steep, leading to a concentration of draws in that part of the prior distribution. We replace this bijective mapping with an iterative prior sampling. This modification allows for a more thorough and stable exploration of the parameter space.

To implement DIME, we set $\nu = 5$ and $\gamma = 2.38\sqrt{2\,\text{size}(\theta)}$, following ter Braak and Vrugt (2008), which yields a value of 0.486. Following Boehl (2024), we set $\rho = 0.999$ and $\xi = 0.05$, as this choice achieved faster convergence in test runs compared with the default $\xi = 0.10$. The disturbance term ϵ_i^j is sampled from a mean-zero normal distribution with variance 1×10^{-5}, consistent with the DIME default. We run 60 chains for 5,000 iterations, retaining 500 as draws from the posterior distribution.

4 Results of the Two-equilibria Model

The log-likelihoods of the ensembles converged after about 1000 iterations as shown in the appendix, so that retaining just 500 draws from the posterior distribution ensures a plausible approximation of the posterior distribution.

4.1 Posterior Parameter Estimates

Table 2 shows the mean, median and the 5^{th} and 95^{th} percentiles of the posterior distribution of the parameter estimates for the United States, the euro area, and Japan together with the prior distributions.

There are two estimated behavioral parameters in the model: the intertemporal elasticity of substitution, α, and the slope of the Phillips curve, κ. The posterior mean estimates of α are 0.06 for the United States, 0.11 for the euro area, and 0.03 for Japan. For all three economies, the data are highly informative, as the posterior means are substantially lower than the prior means, which lie far above the 95^{th} percentile of the posterior distribution. These estimates imply a relatively weak direct response of the output gap to the interest rate gap, consistent with the low consumption response to the real interest rate documented by Hall (1988). By comparison, the meta-study by Havranek et al. (2015) reports an average estimate of 0.59 for the United States. For the euro area, no aggregate meta-estimate is available. However, averaging country-level estimates for Germany, France, Italy, and Spain yields an intertemporal elasticity of approximately 0.21. For Japan, Havranek et al. (2015) report an average of 0.9. They emphasize, though, that negative and statistically insignificant estimates are often omitted from reported results. Accounting for publication bias, even a mean macroeconomic estimate near zero is plausible. Overall, there is substantial heterogeneity in empirical estimates, and several studies argue that low values may may be more consistent with the observed properties of consumption and the Euler equation (e.g., Kilponen et al., 2022).

The posterior mean estimates of the slope of the Phillips curve, κ, are 0.07 for the United States, 0.16 for the euro area, and 0.31 for Japan. The data are informative for all three economies: for the United States and the euro area, both the posterior means and the 95^{th} percentiles lie below the prior means, while for Japan the posterior mean and the 5^{th} percentile lie above. These estimates

Table 2: Posterior Estimates: Two-equilibria model

		Prior distribution			Posterior distribution			
		Distr.	Para (1)	Para (2)	Mean	Median	5%	95%
United States								
Intertemporal elasticity of substitution	α	$\mathcal{G}$	0.50	0.50	0.06	0.06	0.02	0.11
Slope of Phillips curve	κ	$\mathcal{G}$	0.20	0.10	0.07	0.07	0.04	0.11
Monetary policy reaction to inflation	g_π	$\mathcal{G}$	1.50	0.25	1.82	1.78	1.37	2.34
Monetary policy reaction to output gap	g_y	$\mathcal{G}$	0.50	0.25	0.62	0.56	0.12	1.46
Interest rate smoothing	ρ	$\mathcal{B}$	0.50	0.20	0.90	0.90	0.86	0.94
Shock processes								
AR(1) coeff. of supply shock	ρ_u	$\mathcal{B}$	0.50	0.20	0.21	0.20	0.14	0.26
AR(1) coeff. of demand shock	ρ_v	$\mathcal{B}$	0.50	0.20	0.38	0.38	0.17	0.67
Std. dev. of supply shock	σ_u	$\mathcal{IG}$	0.10	2.00	0.0956	0.0979	0.0917	0.0998
Std. dev. of demand shock	σ_v	$\mathcal{IG}$	0.10	2.00	0.0332	0.0093	0.0026	0.0979
Natural rate processes								
AR(1) coeff. of short-run natural rate	ρ_r	$\mathcal{B}$	0.50	0.20	0.32	0.31	0.13	0.50
Std. dev. of short-run nat. rate shock	σ_ϵ	$\mathcal{IG}$	0.10	2.00	0.0009	0.0009	0.0005	0.0012
Std. dev. of long-run nat. rate shock	σ_η	$\mathcal{IG}$	0.10	2.00	0.0729	0.0718	0.0569	0.0959
Euro area								
Intertemporal elasticity of substitution	α	$\mathcal{G}$	0.50	0.50	0.11	0.10	0.05	0.18
Slope of Phillips curve	κ	$\mathcal{G}$	0.20	0.10	0.16	0.14	0.10	0.26
Monetary policy reaction to inflation	g_π	$\mathcal{G}$	1.50	0.25	1.72	1.73	1.26	2.26
Monetary policy reaction to output gap	g_y	$\mathcal{G}$	0.50	0.25	0.42	0.40	0.16	0.81
Interest rate smoothing	ρ	$\mathcal{B}$	0.50	0.20	0.94	0.94	0.93	0.95
Shock processes								
AR(1) coeff. of supply shock	ρ_u	$\mathcal{B}$	0.50	0.20	0.36	0.37	0.13	0.64
AR(1) coeff. of demand shock	ρ_v	$\mathcal{B}$	0.50	0.20	0.35	0.33	0.15	0.58
Std. dev. of supply shock	σ_u	$\mathcal{IG}$	0.10	2.00	0.0219	0.0060	0.0017	0.0959
Std. dev. of demand shock	σ_v	$\mathcal{IG}$	0.10	2.00	0.0529	0.0495	0.0083	0.0983
Natural rate processes								
AR(1) coeff. of short-run natural rate	ρ_r	$\mathcal{B}$	0.50	0.20	0.35	0.36	0.15	0.55
Std. dev. of short-run nat. rate shock	σ_ϵ	$\mathcal{IG}$	0.10	2.00	0.0012	0.0012	0.0007	0.0020
Std. dev. of long-run nat. rate shock	σ_η	$\mathcal{IG}$	0.10	2.00	0.0708	0.0685	0.0507	0.0914
Japan								
Intertemporal elasticity of substitution	α	$\mathcal{G}$	0.50	0.50	0.03	0.03	0.02	0.05
Slope of Phillips curve	κ	$\mathcal{G}$	0.20	0.10	0.31	0.30	0.22	0.42
Monetary policy reaction to inflation	g_π	$\mathcal{G}$	1.50	0.25	1.32	1.31	1.04	1.70
Monetary policy reaction to output gap	g_y	$\mathcal{G}$	0.50	0.25	0.38	0.33	0.15	0.67
Interest rate smoothing	ρ	$\mathcal{B}$	0.50	0.20	0.95	0.95	0.94	0.95
Shock processes								
AR(1) coeff. of supply shock	ρ_u	$\mathcal{B}$	0.50	0.20	0.69	0.77	0.28	0.89
AR(1) coeff. of demand shock	ρ_v	$\mathcal{B}$	0.50	0.20	0.16	0.15	0.11	0.24
Std. dev. of supply shock	σ_u	$\mathcal{IG}$	0.10	2.00	0.0075	0.0049	0.0018	0.0228
Std. dev. of demand shock	σ_v	$\mathcal{IG}$	0.10	2.00	0.0947	0.0959	0.0874	0.0994
Natural rate processes								
AR(1) coeff. of short-run natural rate	ρ_r	$\mathcal{B}$	0.50	0.20	0.38	0.37	0.19	0.67
Std. dev. of short-run nat. rate shock	σ_ϵ	$\mathcal{IG}$	0.10	2.00	0.0007	0.0007	0.0005	0.0009
Std. dev. of long-run nat. rate shock	σ_η	$\mathcal{IG}$	0.10	2.00	0.0389	0.0381	0.0298	0.0523

Notes: The prior distribution types are abbreviated as Gamma ($\mathcal{G}$), Beta ($\mathcal{B}$), and Inverse Gamma ($\mathcal{IG}$). Para (1) and Para (2) list the mean and standard deviation for the Gamma and Beta distributions, respectively. For the Inverse Gamma distribution, Para (1) denotes the shape parameter and Para (2) the scale parameter.

are consistent with model-based results in the literature. For example, Schorfheide (2008) report estimates for the United States ranging from zero to 0.77 (excluding the outlier of 4.15 in Canova 2009), placing the estimates of all three economies well within this range. Limited-information estimates are often only slightly positive and the literature also emphasizes the high degree of uncertainty surrounding the slope of the Phillips curve (see, e.g., Nakamura and Steinsson, 2013; Mavroeidis et al., 2014; Eser et al., 2020; Furlanetto and Lepetit, 2024). The estimates for the United States and the euro area are thus squarely within the range reported in previous studies, and even the higher estimate for Japan is plausible and consistent with the broader evidence. Importantly, the slope of the Phillips curve measures only the immediate impact of the output gap on inflation. Additional effects can arise through changes in inflation expectations, which may be stronger here than in conventional models with anchored expectations.

The estimates for the monetary policy rule parameters fall within the range typically reported in comparable studies for all three economies. The posterior mean of the inflation response is somewhat higher in the United States and the euro area with values of 1.82 and 1.72 than the prior of 1.50, with the posterior distribution shifted upward, while in Japan the posterior remains close to the prior. For the output gap response, the posterior means are close to the prior across all three economies, indicating that the data are not informative. By contrast, the data are highly informative for the interest rate smoothing coefficient: the posterior means lie between 0.90 and 0.95 with tight posterior distributions, reflecting the high degree of interest rate smoothing usually found in empirical estimates of monetary policy rules.

The data are highly informative about the shock processes. For all three economies and virtually all shocks, posterior means of the AR(1) coefficients and shock standard deviations lie below prior means, and posterior distributions are noticeably tighter. The only exceptions are the AR(1) coefficient of the United States demand shock and that of the Japanese supply shock, whose posterior means remain close to the prior. The prior mean of the autocorrelation coefficient is 0.5 for all shocks, while posterior means fall in the range 0.16–0.69. The prior mean of the innovation standard deviation is 0.1, while posterior estimates range from 0.01 to 0.1, except for the short-run natural rate shock, whose posterior is markedly smaller. Because the long-run natural rate is observed whereas the short-run component is latent, and given the high persistence of the former, the estimates imply that transitory natural rate shocks have negligible quantitative relevance.

Overall, the parameter estimates appear plausible. Differences in comparison to previous studies could be caused by the possibility of inflation deanchoring, which leads to substantially different model dynamics (see, e.g., Aruoba et al., 2018; Lansing, 2021).

4.2 Equilibrium Transition Probabilities

We analyze the endogenous forecast weights μ_t using the estimated model, following the *reverse engineering* approach of Lansing and Markiewicz (2018), Gelain et al. (2018), and Lansing (2021).[3] For each period t, we draw from the posterior distribution and compute μ_t via equation (10), which requires one-step-ahead expectations from the target and low-inflation equilibria for $t-9$ to $t-2$. These expectations are obtained by substituting the shock realizations and observables into the model solutions for both equilibria. Conditional on μ_t, the transition-model expectations are computed using equation (9) and combined with observables to infer the shock realizations for period t via the model equations in Section 2.1. For $t = 1$ to 8, we set $\mu_t = 1$, providing the initial shock realizations needed to compute μ_t in subsequent periods. We perform the reverse engineering exercise by randomly drawing 100 parameters from the posterior parameter distribution to account for the uncertainty in the parameter estimates. The results are shown in Figure 1.

The plots on the left show the evolution of μ_t over time, where $\mu_t = 1$ indicates that agents assign full probability to the target equilibrium, and $\mu_t = 0$ indicates full probability on the low-inflation equilibrium. Intermediate values correspond to a mixture of the two local equilibria. We report the median posterior estimates of μ_t along with 90% probability bands. The probability assigned to each equilibrium at each point in time depends on the relative one-step-ahead forecasting accuracy of the target and low-inflation forecast rules for inflation and the output gap over the preceding eight quarters. To illustrate the sources of time variation in μ_t, the right-hand plots show the inflation series together with the corresponding endpoints of the two inflation forecasts. We focus on inflation because the endpoints differ markedly between equilibria: in the target equilibrium, the inflation endpoint equals π^*, whereas in the low-inflation equilibrium it equals $-r_t^*$. By contrast, differences in the output gap endpoints are small. For the target equilibrium, the endpoint is $(1-\beta)\pi^*/\kappa$, and for the low-inflation equilibrium it is $(1-\beta)(-r_t^*)/\kappa$, which are both approximately zero given $\beta = 0.99$.

[3] A particle smoother could be employed instead; however, the resulting μ_t estimates were highly uncertain and volatile, making them difficult to interpret.

Figure 1: Target Probabilities and Inflation Endpoints

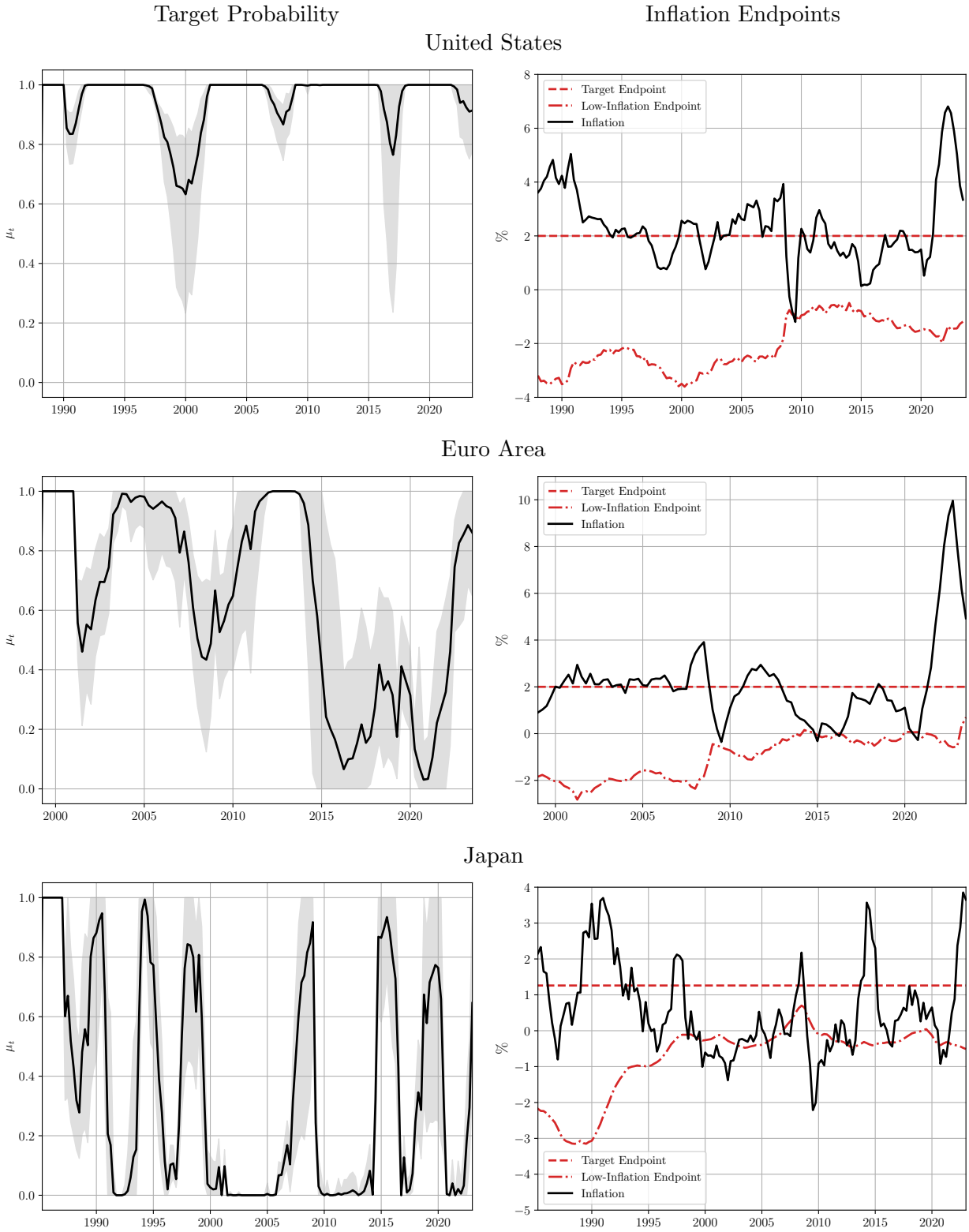

Notes: Left panels: The black solid line depicts the median target probability. The shaded area describes the interval between the 5^{th} and 95^{th} percentile. Right panels: The black solid line describes annualized quarterly inflation. The upper red dashed line represents the inflation target endpoint, which is equal to π^*. The lower red dashed-dotted line represents the low-inflation endpoint, which is equal to $-r_t^*$.

United States. The U.S. economy remained predominantly in the target equilibrium, with μ_t never falling below 60%. This reflects inflation fluctuating around the target over the sample, with only occasional more persistent declines below it. Declines in μ_t in the late 1990s, around the 2008–09 global financial crisis, and around 2016 correspond to such periods. Early- and late-sample deviations occurred when inflation was above target but trending downward. Low-inflation equilibrium forecasts project a faster decline in inflation, inducing moderate reductions in μ_t even when inflation remains above target. Thus, the forecast-switching mechanism appears somewhat sensitive to short-term inflation declines, though associated reductions in the target probability remain limited. Overall, the results corroborate Aruoba et al. (2018), confirming that the United States remained in the target regime, and align with Lansing (2021), who reports target-equilibrium probabilities exceeding 60% throughout the sample.

Euro area. For the euro area, variation in μ_t is much larger than in the United States, underscoring the relevance of equilibrium transitions. The sharpest decline to near zero occurred in 2014/15, when inflation fell to zero and r_t^* also dropped toward zero, so that the low-inflation endpoint nearly coincided with actual inflation. This episode lasted until 2020, interrupted only by a temporary rise of inflation toward target that briefly lifted μ_t, though it remained below 50%. Even accounting for estimation uncertainty, the model clearly indicated a de-anchoring of inflation expectations in line with Nautz et al. (2017), Natoli and Sigalotti (2018), Corsello et al. (2021) and Christoffel and Farkas (2025). From 2021 onward, the euro area economy returned to the target equilibrium. μ_t remained slightly below 100%, however, as expectations continued to assign weight to the low-inflation equilibrium, which implied faster disinflation after 2022.

Beyond the 2015–2020 episode, the joint drop in inflation and the natural rate during the global financial crisis also raised the low-inflation endpoint and reduced μ_t toward 50%, suggesting the economy was best characterized as a mixture of equilibria. Around 2001, μ_t also dipped temporarily as inflation slightly exceeded target before converging back. In this case, the forecasts of the two equilibria diverged only marginally, so weight was placed on both. This highlights that μ_t should not be interpreted mechanically: a decline in μ_t is informative only if accompanied by persistently below-target inflation.

Japan. For Japan, transitions to a low-inflation equilibrium are even more relevant than for the euro area. Japan transitioned around 1996, when inflation fell below zero and the natural

interest rate declined from 4% to 1%, narrowing the distance between the target and the low-inflation endpoint.[4] It then remained in the low-inflation equilibrium until the end of the sample, interrupted only by temporary increases in μ_t during short-lived inflation spikes. The sensitivity of μ_t to such spikes follows mechanically from the small gap between the equilibrium endpoints, as the pre-2013 inflation target of only 1% combined with a natural interest rate that fell to zero in the late 1990s. Apart from these spikes, μ_t converged to zero with narrow uncertainty bands, reflecting that from the late 1990s until the launch of *Abenomics* around 2012, inflation remained near the low-inflation endpoint, consistent with Aruoba et al. (2018).

5 Comparison to Single-equilibrium Models

The analysis so far has shown that, under the assumed RMSFE minimization procedure, agents choose a time-varying μ_t in all three economies. In this section, we assess formally whether the equilibrium-transition model with this expectation formation mechanism provides a better fit than single-equilibrium models, in which $\mu_t = 1$ or $\mu_t = 0$ for all t, replacing the time-varying μ_t chosen via equation (10). The target-equilibrium model corresponds to $\mu_t = 1$, with expectations anchored at the target long-run endpoint. The ELB may bind occasionally, but once shocks fade, inflation returns to target and interest rates turn positive. This specification is most relevant for the United States, where μ_t remained close to one throughout the sample. The low-inflation-equilibrium model corresponds to $\mu_t = 0$, with expectations anchored at the low-inflation long-run endpoint. The ELB may temporarily cease to bind, but once shocks dissipate, inflation converges to the low-inflation endpoint $\pi_t^L = -r_t^*$ and the ELB binds in the long run. This specification is most relevant for Japan, where μ_t frequently took values near zero. For estimation, we apply the same priors, sample periods, and methodology as in the transition model.

5.1 Model Selection Metrics

Table 3 reports the log marginal data densities, computed using the Modified Harmonic Mean Estimator of Geweke (1999), for the transition model, the target-equilibrium model, and the low-inflation model. Model comparison is based on the Bayes factor, defined as the ratio of marginal

[4]The previous decrease of μ_t around 1992 arises due to the persistent decline of inflation starting from above the inflation target, rather from trantitioning to a low-inflation equilibrium.

likelihoods. Under equal prior probabilities, the Bayes factor coincides with the posterior odds ratio. We also report the Kass–Raftery statistic, defined as twice the log of the Bayes factor.

Table 3: Model Selection Metrics

Log Marginal Data Density			
	Transition Model	**Target Model**	**Low-Inflation Model**
United States	1977.44	1130.62	1104.14
Euro Area	1338.06	1007.78	952.72
Japan	2272.47	1779.54	1799.48

Bayes Factor / Kass-Raftery Statistic			
	Transition vs. Target	**Transition vs. Low-Inflation**	**Target vs. Low-Inflation**
United States			
Bayes Factor	$> 10^{100}$	$> 10^{100}$	3.16×10^{11}
Kass-Raftery	1681.65	1746.61	64.97
Euro Area			
Bayes Factor	$> 10^{100}$	$> 10^{100}$	8.17×10^{23}
Kass-Raftery	660.55	770.70	110.12
Japan			
Bayes Factor	$> 10^{100}$	$> 10^{100}$	2.18^{-9}
Kass-Raftery	985.86	945.98	-39.89

Comparing the transition equilibrium model with the two single-equilibrium alternatives yields extremely large Bayes factors and Kass–Raftery statistics across all three economies. Using the terminology of Kass and Raftery (1995), this provides 'strong evidence' in favor of the transition equilibrium specification. The result is particularly noteworthy for the United States, where the estimated values of μ_t reported above remain close to unity.

The dominance of the transition equilibrium model can be understood by noting that the log marginal data density is the sum of one-step-ahead predictive scores. Forecasts from single-equilibrium DSGE models typically imply a quick return to steady state after shocks (see, e.g., Wickens, 2014). This reversion is even faster in the small-scale models used here than in larger Smets and Wouters (2007)-type models. When downward deviations from steady state are persistent, the transition model delivers more accurate forecasts. The RMSFE minimization in equation (10) lowers μ_t, which reduces inflation and output gap forecasts and, in turn, interest rate forecasts. If these variables are persistent, this adjustment improves one-step-ahead predictive accuracy. The transition equilibrium model therefore captures persistence in the data more effectively than single-equilibrium models. It can thus fit economies with prolonged periods of low inflation and low interest rates, as in the euro area and Japan, as well as cases with only temporary downward deviations, as in the United States.

When comparing the target and low-inflation equilibria, the differences are less pronounced. For the United States and the euro area, however, the Bayes factors and Kass–Raftery statistics remain sufficiently large to constitute 'strong evidence' in favor of the target equilibrium model. In contrast, for Japan the Bayes factor falls below one, indicating that the low-inflation equilibrium is preferred. The magnitude of the difference is large enough to be classified as 'strong evidence' according to Kass and Raftery (1995). This result quantitatively confirms that the Japanese economy has been in a different equilibrium—commonly referred to as "Japanification"—since the late 1990s or early 2000s. Hence, when restricting attention to single-equilibrium frameworks, the standard New Keynesian model is not appropriate for Japan.

The superior fit of the transition model is evident in the joint distribution of inflation and the interest rate—the two variables for which the long-run endpoints differ most. Figure 2 illustrates this for the euro area. Analogous figures for the United States and Japan are provided in the appendix. The lower-right panel shows the distribution in the data, which reflects periods when the ELB binds and inflation is volatile, as well as periods when the ELB does not bind and inflation is more tightly centered around the target. Simulations with $\mu_t = 0$ (top right) reproduce the former, while those with $\mu_t = 1$ (top left) replicate the latter. The transition model with time-varying μ_t (lower left) provides the closest overall match, as it adapts to episodes in which either the target equilibrium or the low-inflation equilibrium is more relevant, and even captures cases best described as a mixture of the two. The overlap of the contour plots for the target and low-inflation equilibria indicates that such cases are empirically important.

5.2 Posterior Estimates of Single-equilibrium Models

Table 4 reports posterior estimates for the single-equilibrium models. For all three economies, several parameter estimates differ markedly from those of the transition model. We regard differences as significant when the posterior mean of one model lies outside the 5^{th}–95^{th} percentile range of the other. Consistent with the model selection metrics discussed above, the subsequent analysis compares the target and transition models for the United States and the euro area, and the low-inflation and transition models for Japan.

For the intertemporal elasticity of substitution, target-equilibrium values for the United States and euro area far exceed transition-equilibrium estimates. Because the transition model is strongly

Table 4: Posterior Estimates: Single Equilibrium Models

		Target Equilibrium Model				Low-Inflation Equilibrium Model			
		Mean	Median	5%	95%	Mean	Median	5%	95%
United States									
Intertemp. elast. of substitution	α	0.21	0.17	0.10	0.42	0.00	0.00	0.00	0.01
Slope of Phillips curve	κ	0.17	0.16	0.08	0.32	0.15	0.15	0.06	0.24
Mon. pol. reaction to inflation	g_π	1.60	1.59	1.09	2.24	1.75	1.78	1.21	2.30
Mon. pol. reaction to output gap	g_y	2.09	2.16	1.57	2.49	1.55	1.58	0.66	2.33
Interest rate smoothing	ρ	0.74	0.76	0.58	0.85	0.92	0.92	0.88	0.95
Shock processes									
AR(1) coeff. of supply shock	ρ_u	0.11	0.10	0.10	0.11	0.62	0.65	0.35	0.85
AR(1) coeff. of demand shock	ρ_v	0.29	0.29	0.12	0.54	0.72	0.71	0.65	0.81
Std. dev. of supply shock	σ_u	0.0968	0.0970	0.0931	0.0997	0.0699	0.0743	0.0377	0.0888
Std. dev. of demand shock	σ_v	0.0120	0.0071	0.0018	0.0338	0.0713	0.0752	0.0364	0.0966
Natural rate processes									
AR(1) coeff. short-run natural rate	ρ_r	0.77	0.77	0.61	0.90	0.46	0.44	0.22	0.71
Std. dev. short-run nat. rate shock	σ_ϵ	0.0793	0.0814	0.0470	0.0962	0.0636	0.0615	0.0414	0.0945
Std. dev. long-run nat. rate shock	σ_η	0.0014	0.0014	0.0010	0.0019	0.0014	0.0013	0.0009	0.0020
Euro Area									
Intertemp. elast. of substitution	α	0.78	0.79	0.60	0.92	0.03	0.02	0.00	0.08
Slope of Phillips curve	κ	0.10	0.09	0.06	0.14	0.10	0.10	0.04	0.16
Mon. pol. reaction to inflation	g_π	1.41	1.33	1.03	1.88	1.81	1.84	1.34	2.32
Mon. pol. reaction to output gap	g_y	1.24	1.18	0.86	1.92	0.60	0.56	0.22	1.14
Interest rate smoothing	ρ	0.57	0.56	0.46	0.72	0.93	0.93	0.89	0.95
Shock processes									
AR(1) coeff. of supply shock	ρ_u	0.11	0.11	0.10	0.12	0.59	0.61	0.29	0.78
AR(1) coeff. of demand shock	ρ_v	0.32	0.32	0.20	0.46	0.79	0.78	0.73	0.86
Std. dev. of supply shock	σ_u	0.0972	0.0973	0.0942	0.0999	0.0700	0.0732	0.0386	0.0914
Std. dev. of demand shock	σ_v	0.0643	0.0661	0.0245	0.0943	0.0656	0.0674	0.0281	0.0960
Natural rate processes									
AR(1) coeff. short-run natural rate	ρ_r	0.85	0.86	0.74	0.90	0.46	0.46	0.13	0.81
Std. dev. short-run nat. rate shock	σ_ϵ	0.0456	0.0435	0.0343	0.0618	0.0583	0.0562	0.0383	0.0871
Std. dev. long-run nat. rate shock	σ_η	0.0017	0.0017	0.0011	0.0026	0.0017	0.0016	0.0012	0.0023
Japan									
Intertemp. elast. of substitution	α	0.02	0.02	0.01	0.03	0.02	0.02	0.01	0.04
Slope of Phillips curve	κ	0.34	0.34	0.27	0.42	1.09	1.09	0.72	1.60
Mon. pol. reaction to inflation	g_π	1.83	1.83	1.61	2.08	1.58	1.55	1.20	2.05
Mon. pol. reaction to output gap	g_y	0.19	0.17	0.11	0.30	0.57	0.53	0.17	1.10
Interest rate smoothing	ρ	0.92	0.92	0.90	0.93	0.94	0.94	0.93	0.95
Shock processes									
AR(1) coeff. of supply shock	ρ_u	0.26	0.25	0.13	0.44	0.87	0.87	0.84	0.90
AR(1) coeff. of demand shock	ρ_v	0.10	0.10	0.10	0.11	0.58	0.58	0.36	0.81
Std. dev. of supply shock	σ_u	0.0124	0.0101	0.0021	0.0308	0.0914	0.0923	0.0818	0.0991
Std. dev. of demand shock	σ_v	0.0988	0.0989	0.0979	0.0998	0.0709	0.0798	0.0221	0.0969
Natural rate processes									
AR(1) coeff. short-run natural rate	ρ_r	0.89	0.89	0.88	0.90	0.49	0.49	0.18	0.78
Std. dev. short-run nat. rate shock	σ_ϵ	0.0908	0.0919	0.0753	0.0986	0.0440	0.0454	0.0261	0.0619
Std. dev. long-run nat. rate shock	σ_η	0.0014	0.0013	0.0010	0.0017	0.0012	0.0012	0.0009	0.0015

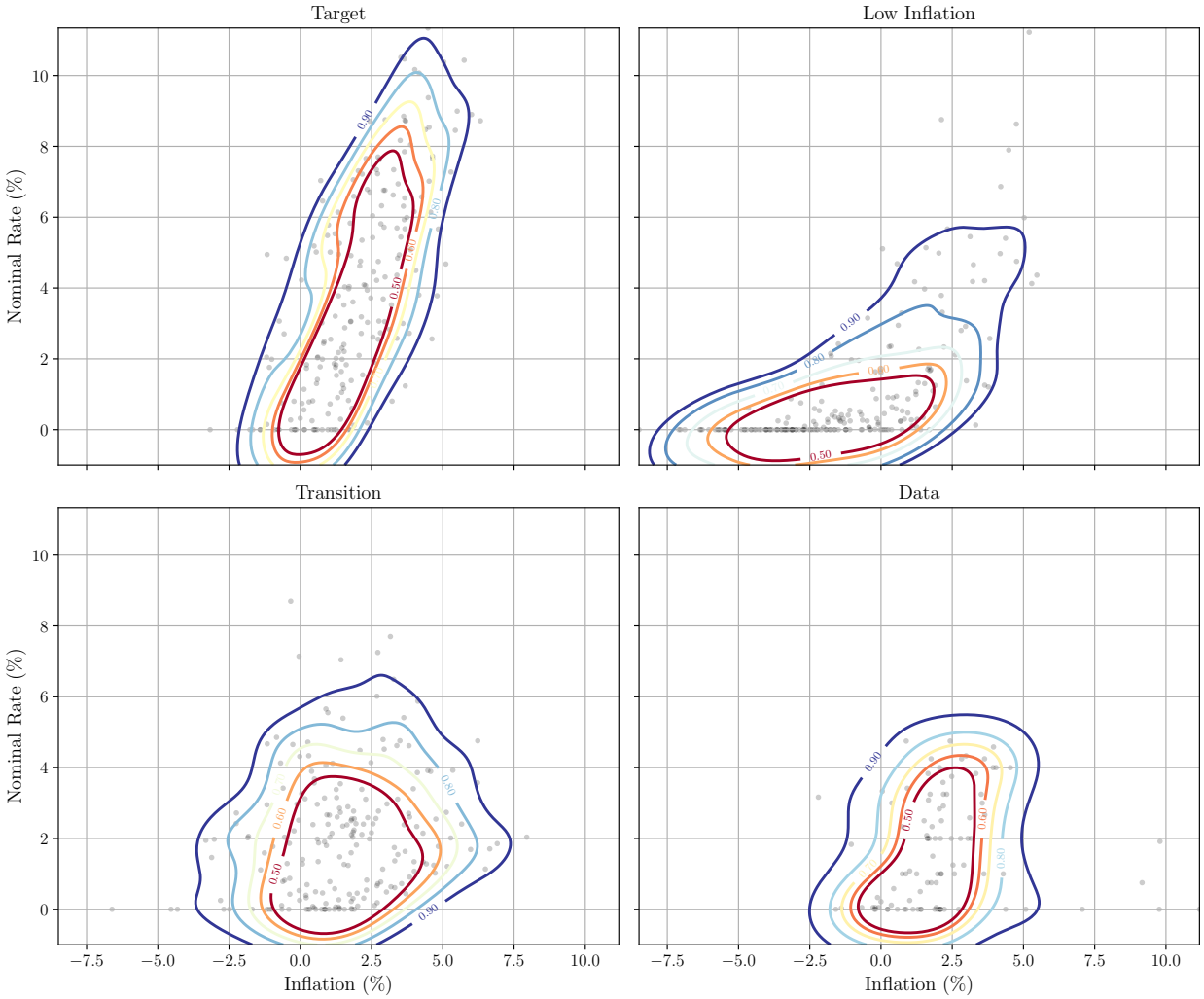

Figure 2: Contour Plots for the Euro Area

Notes: Joint distributions of inflation and nominal interest rates in the target (top left), low-inflation (top right), and transition equilibria (bottom left) compared with the data (bottom right), respectively. Black dots show realizations, contour lines denote kernel density estimates; each contour encloses the indicated share of the probability mass $(50 - 90\%)$.

favored by the data, the target-equilibrium estimates would substantially overstate the output effects of monetary policy. Phillips curve slopes also vary significantly, so that the sensitivity of inflation to the output gap differs substantially across models. The target model yields higher values in the United States but lower ones in the euro area, and for Japan the low-inflation model implies a very steep slope relative to the transition model.

Policy rule parameters show a stronger output-gap response and less interest rate smoothing under the target model, though inflation responses are similar. Only for Japan are estimates consistent across models. Shock process estimates diverge as well for all three economies.

Overall, the posterior estimates highlight substantial differences between the single-equilibrium models and the transition model in key structural parameters, policy parameters, and shock processes. Hence, even in periods when μ_t equals zero or one, the dynamics implied by the transition model may differ from those of the target and low-inflation models.

6 Robustness Checks

We conduct two robustness checks, first using an alternative well-established sampler, and second examining whether core rather than headline inflation improves the identification of sustained equilibrium transitions.

6.1 DEMC Sampler

To validate the estimates, we re-estimate the transition equilibrium model for all three economies using a different sampling algorithm. Specifically, we employ the well-established DEMC sampler of ter Braak and Vrugt (2008). The DEMC sampler is nested within the DIME sampler and is obtained by setting ξ, the probability that a chain is assigned to the global transition kernel, to zero, so that all chains are sampled from the local transition kernel via DEMC. Apart from using the DEMC sampler, the estimation setup is identical to the original specification.

The posterior estimates are reported in the appendix. Posterior means based on the DEMC sampler are generally similar to those obtained with the DIME sampler. While the DIME sampler is designed to avoid convergence to local maxima, the similarity of results indicates that the DEMC sampler also converges to the global maximum. The posterior distributions under DEMC are, however, wider, reflecting the absence of the DIME sampler's global transition kernel, which accounts for the full distribution of chains.

6.2 Core Inflation

Temporary declines in inflation toward the low-inflation equilibrium, or short-lived rebounds to target driven by energy price volatility, may mask more persistent shifts between equilibria. To mitigate this concern, we re-estimated the model using core rather than headline inflation. The resulting parameter estimates (reported in the appendix) are broadly similar, though the Phillips

curve slope is lower for the euro area and Japan, and the shock processes display some differences in Japan.

Figure 3 shows the estimates of μ_t. They are somewhat smoother, with broadly unchanged transition timing, but exhibit wider uncertainty bands for the euro area and Japan. The amplitude of movements is larger. For instance, in the euro area the dips of μ_t in 2001 and 2008 reach values around 0.2 rather than 0.5. In Japan, the temporary reversal towards the target equilibrium in 2015 is more pronounced: whereas μ_t briefly peaked at 0.8 with headline inflation, it now rises to nearly 1.0 and remains there for over a year. The greater persistence of core inflation amplifies forecast differences across equilibria, inducing stronger responses of μ_t.

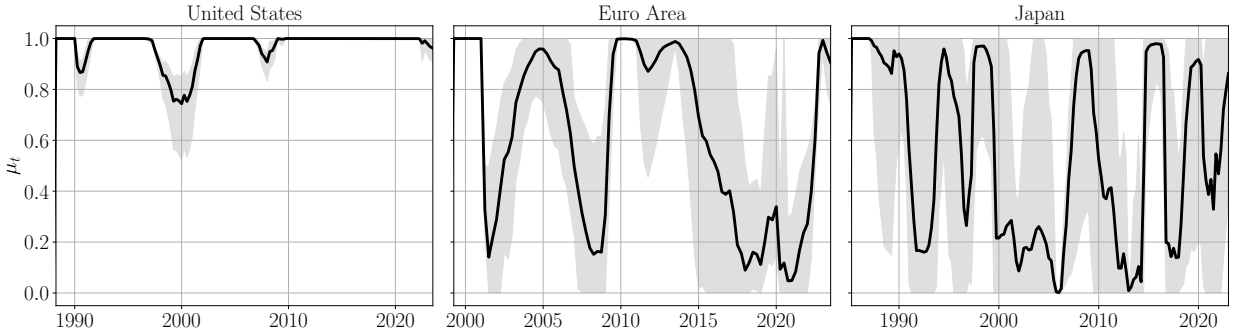

Figure 3: Target Probability under Core Inflation

Overall, the use of core inflation does not provide clear advantages under the current expectation formation mechanism. Avoiding temporary reversals in μ_t would require excluding additional volatile components from inflation. A more promising avenue, however, is to consider alternative expectation formation mechanisms, as discussed in the conclusion.

7 Conclusion

This paper provides new evidence on the importance of modeling transitions between a standard equilibrium with anchored inflation expectations and a low-inflation equilibrium with de-anchored expectations in New Keynesian models with the ELB. We show that such nonlinear models can be successfully estimated using a particle filter. Model selection criteria strongly favor the equilibrium-transition specification over conventional models with anchored expectations and only occasionally binding ELB constraint. These results underscore the importance of policy frameworks that can influence long-run inflation expectations and mitigate de-anchoring risks.

We employ an off-the-shelf model—the only one in the literature with endogenous transitions between a target and a low-inflation equilibrium. Future work could explore alternative expectation formation mechanisms that allow equilibrium transitions. Extending the model to account for both downward and upward deviations of inflation expectations from target could enhance its usefulness in episodes like the recent inflation surge. Such models could continue to be estimated using particle filtering and flexible MCMC sampling, as demonstrated in this paper.

References

An, S. and F. Schorfheide (2007). Bayesian analysis of DSGE models. *Econometric Reviews 26*, 113–172.

Armenter, R. (2018). The perils of nominal targets. *The Review of Economic Studies 85*(1), 50–86.

Aruoba, S. B., P. Cuba-Borda, K. Higa-Flores, F. Schorfheide, and S. Villalvazo (2021). Piecewise-linear approximations and filtering for DSGE models with occasionally-binding constraints. *Review of Economic Dynamics 41*, 96–120.

Aruoba, S. B., P. Cuba-Borda, and F. Schorfheide (2018). Macroeconomic dynamics near the ZLB: A tale of two countries. *Review of Economic Studies 85*, 87–118.

Benhabib, J., S. Schmitt-Grohé, and M. Uribe (2001a). Monetary policy and multiple equilibria. *American Economic Review 91*(1), 167–186.

Benhabib, J., S. Schmitt-Grohé, and M. Uribe (2001b). The perils of Taylor rules. *Journal of Economic Theory 96*, 40–69.

Bilbiie, F. O. (2022). Neo-Fisherian policies and liquidity traps. *American Economic Journal: Macroeconomics 14*(4), 378–403.

Boehl, G. (2022). Efficient solution and computation of models with occasionally binding constraints. *Journal of Economic Dynamics and Control 143*, 104523.

Boehl, G. (2024). DIME MCMC: A swiss army knife for Bayesian Inference. Working paper, University of Bonn.

Boehl, G. and F. Strobel (2024). Estimation of DSGE models with the effective lower bound. *Journal of Economic Dynamics and Control 158*, 104784.

Canova, F. (2009). What explains the Great Moderation in the U.S.? A structural analysis. *Journal of the European Economic Association 7*(4), 697–721.

Carvalho, C., S. Eusepi, E. Moench, and B. Preston (2023). Anchored inflation expectations. *American Economic Journal: Macroeconomics 15*(1), 1–47.

Cho, S., T. M. Mertens, and J. C. Williams (2025). The zero lower bound remains a medium-term risk. *FRBSF Economic Letter* (July 7).

Christoffel, K. and M. Farkas (2025). Managing the risks of inflation expectation de-anchoring. Working Paper Series 3082, European Central Bank.

Corsello, F., S. Neri, and A. Tagliabracci (2021). Anchored or de-anchored? That is the question. *European Journal of Political Economy 69*, 1–19.

Cuba-Borda, P. and S. R. Singh (2024). Understanding persistent ZLB: Theory and assessment. *American Economic Journal: Macroeconomics 16*(3), 389–416.

Eser, F., P. Karadi, P. R. Lane, L. Moretti, and C. Osbat (2020). The Phillips curve at the ECB. *The Manchester School 88*(S1), 50–85.

Farmer, R. E., V. Khramov, and G. Nicolò (2015). Solving and estimating indeterminate DSGE models. *Journal of Economic Dynamics and Control 54*, 17–36.

Fernández-Villaverde, J. and J. F. Rubio-Ramírez (2007). Estimating macroeconomic models: A likelihood approach. *The Review of Economic Studies 74*(4), 1059–1087.

Fischer, J. J. (2023). De-anchored inflation expectations and monetary policy. Working paper, European University Institute.

Furlanetto, F. and A. Lepetit (2024). The slope of the Phillips curve. Finance and Economics Discussion Series 2024-04, Washington: Board of Governors of the Federal Reserve System.

Gelain, P., K. J. Lansing, and G. J. Natvik (2018). Explaining the boom–bust cycle in the U.S. housing market: A reverse-engineering approach. *Journal of Money, Credit and Banking 50*(8), 1751–1783.

Geweke, J. (1999). Using simulation methods for bayesian econometric models: inference, development, and communication. *Econometric Reviews 18*(1), 1–73.

Grishchenko, O., S. Mouabbi, and J. P. Renne (2019). Measuring inflation anchoring and uncertainty: A US and euro area comparison. *Journal of Money, Credit and Banking 51*(5), 1053–1096.

Guerrieri, L. and M. Iacoviello (2015). Occbin: A toolkit for solving dynamic models with occasionally binding constraints easily. *Journal of Monetary Econometrics 70*, 22–38.

Gust, C., E. Herbst, D. López-Salido, and M. E. Smith (2017). The empirical implications of the interest rate lower bound. *American Economic Review 107*(7), 1971–2006.

Hall, R. E. (1988). Intertemporal substitution in consumption. *Journal of Political Economy 96*(2), 339–357.

Havranek, T., R. Horvath, Z. Irsova, and M. Rusnak (2015). Cross-country heterogeneity in intertemporal substitution. *Journal of International Economics 96*(1), 100–118.

Herbst, E. and F. Schorfheide (2016). Bayesian estimation of DSGE models. *Econometric Reviews 35*, 33–60.

Herbst, E. and F. Schorfheide (2019). Tempered particle filtering. *Journal of Econometrics 210*(1), 26–44.

Holden, T. (2016). Computation of solutions to dynamic models with occasionally binding constraints. Working Paper.

Holston, K., T. Laubach, and J. C. Williams (2017). Measuring the natural rate of interest: International trends and determinants. *Journal of International Economics 108*, 59–75.

Hommes, C. H. and W. A. Brock (1997). A rational route to randomness. *Econometrica 65*(5), 1059–1095.

Kass, R. E. and A. E. Raftery (1995). Bayes factors. *Journal of the American Statistical Association 90*(430), 773–795.

Kilponen, J., J. Vilmunen, and O. Vähämaa (2022). Revisiting intertemporal elasticity of substitution in a sticky price model. *Journal of Economic Dynamics and Control 144*, 104498.

Kulish, M., J. Morley, and T. Robinson (2017). Estimating DSGE models with zero interest rate policy. *Journal of Monetary Economics 88*, 35–49.

Lansing, K. J. (2021). Endogenous forecast switching near the zero lower bound. *Journal of Monetary Economics 117*, 153–169.

Lansing, K. J. and A. Markiewicz (2018). Top incomes, rising inequality and welfare. *The Economic Journal 128*(608), 262–297.

Laubach, T. and J. C. Williams (2003). Measuring the natural rate of interest. *Review of Economics and Statistics 85*(4), 1063–1070.

Mavroeidis, S., M. Plagborg-Møller, and J. H. Stock (2014). Empirical evidence on inflation expectations in the New Keynesian Phillips curve. *Journal of Economic Literature 52*(1), 124–88.

Mertens, K. R. S. M. and M. O. Ravn (2014). Fiscal policy in an expectations-driven liquidity trap. *Review of Economic Studies 81*, 1637–1667.

Nakamura, E. and J. Steinsson (2013). Price rigidity: Microeconomic evidence and macroeconomic implications. NBER Working Paper 18705.

Nakano, S., Y. Sukioka, and H. Yamamoto (2024). Recent developments in measuring the natural rate of interest. Bank of Japan Working Paper 24-E-12.

Nakata, T. and S. Schmidt (2022). Expectations-driven liquidity traps: Implications for monetary and fiscal policy. *American Economic Journal: Macroeconomics 14*(4), 68–103.

Natoli, F. and L. Sigalotti (2018). Tail co-movement in inflation expectations as an indicator of anchoring. *International Journal of Central Banking 14*(1), 35–71.

Nautz, D., L. Pagenhardt, and T. Strohsal (2017). The (de-) anchoring of inflation expectations: New evidence from the euro area. *The North American Journal of Economics and Finance 40*, 103–115.

Richter, A. W. and N. A. Throckmorton (2016). Is Rotemberg pricing justified by macro data? *Economics Letters 149*, 44–48.

Schmitt-Grohé, S. and M. Uribe (2017). Liquidity traps and jobless recoveries. *American Economic Journal: Macroeconomics 9*(1), 165–204.

Schorfheide, F. (2008). DSGE model-based estimation of the New Keynesian Phillips Curve. *FRB Richmond Economic Quarterly 94*(4), 397–433.

Smets, F. and R. Wouters (2007). Shocks and frictions in US business cycles: A Bayesian DSGE approach. *American Economic Review 97*(3), 586–606.

Strohsal, T., R. Melnick, and D. Nautz (2016). The time-varying degree of inflation expectations anchoring. *Journal of Macroeconomics 49*, 62–71.

ter Braak, C. J. F. and J. A. Vrugt (2008). Differential evolution Markov chain with snooker updater and fewer chains. *Statistics and Computing 18*, 435–446.

Wickens, M. (2014). How useful are DSGE macroeconomic models for forecasting? *Open Economies Review 25*(1), 171–19.